Experimental investigation on thermal conductivity of surfactant-less aluminium oxide (Al₂O₃) in water nanofluid using acoustic velocity measurements

Sayantan Mukherjee[1], Purna Chandra Mishra[1,]*, Paritosh Chaudhuri[2,3] and Shanta Chakrabarty[1]

[1]Thermal Research Laboratory, School of Mechanical Engineering, Kalinga Institute of Industrial Technology (KIIT) Deemed to be University, Bhubaneswar 751 024, India
[2]Institute for Plasma Research, Bhat, Gandhinagar 382 428, India
[3]Homi Bhabha National Institute, Anushaktinagar, Mumbai 400 094, India

The thermal conductivity of Al₂O₃–water nanofluid (NF) was investigated in this study utilizing ultrasonic velocity. The change in thermal conductivity was calculated by increasing the weight fraction from 0.01% to 1% for every 10°C elevation in the temperature range of 25–65°C. The thermal conductivity of NF augmented with an enhancement in nanoparticle concentration and rise in temperature. The thermal conductivity of NF was higher than that of basefluid. Finally, the experimental results were compared with classical thermal conductivity models and the thermal conductivity enhancement coefficient was further used to investigate thermal conductivity augmentation.

Keywords: Nanofluid, nanoparticles, thermal conductivity, ultrasonic velocity.

IN the present era of rapid advancement in materials technology and visible growth in the energy crisis, researchers have started to apply new materials as working fluids of high thermal conductivity for heat transfer applications[1]. Choi et al.[2] were first to report that dispersion of highly conductive nanoparticles in traditional basefluids such as water, glycols or oils could be a way to increase their heat transfer capability. They coined the novel class of heat transfer fluid as 'nanofluid (NF)'. After the pioneering research work on NF, researchers were motivated to execute various studies to explore the various aspects of NF. According to the report of Ali et al.[3] NFs showed enhancement in several thermal and heat transport properties that are different from the basefluids. An anomalous intensification in the thermal conductivity is one of those properties. For example, the poor thermal conductivity of oil or ethylene glycol can be improved by 150% and 40% respectively, by dispersing Cu nanoparticles or carbon nanotubes (CNTs) at less than 1% vol. fraction[4,5].

Tawfik et al.[6] had applied different experimental techniques and instruments to measure the enhancement in thermal conductivity of NFs. However, there is an inconsistency among the measured thermal conductivity data[7]. Contemporary literature report about the strong dependency of thermal conductivity of NFs on nanoparticle material, morphology, stability, concentration and temperature[8–10]. However, issues of stability and pumping power enhancement get amplified at high concentrations. Besides this, the thermal conductivity enhancement (TCE) in NFs is in the order of magnitude better than the predictions by well-established classical theories.

Research on NFs is still in an infant stage. Thermal conductivity data are of course very important to understand the heat transfer performance of NFs. Various methods have been developed so far in order to measure the thermal conductivity of NFs. However, estimation of the thermal conductivity of NFs using acoustic velocity measurement is novel but less addressed. Thus, the primary goal of our research is to present the measurement of thermal conductivity of aluminium oxide (Al₂O₃)-water NF using sonic velocity in that medium. The effects of nanoparticle concentration and temperature elevation are analysed. Moreover, our aim is to provide guidance to design NFs with better heat transfer performance.

Materials and experiments

Materials

Al₂O₃ nanoparticles (Sisco Research Lab, India) with 92% purity were used in this study. Simple deionized (DI) water was used as basefluid. The selected materials were lab grade and hence, further purification was omitted. The thermo-physical properties of the selected materials are summarized in Table 1. The transmission electron micrograph (TEM) of Al₂O₃ nanoparticles is presented in

*For correspondence. (e-mail: pcmishrafme@kiit.ac.in)

Table 1. Properties of component materials of nanofluid

Materials	Purity	Colour	Particle size (nm)	Morphology	Material phase	Thermal conductivity (Wm^{-1} K^{-1})
Al$_2$O$_3$ nanoparticles	99%	White	20–30	Near spherical	Alpha	40
Water (basefluid)	N/A	Colourless	N/A	N/A	N/A	0.605

N/A, Not applicable.
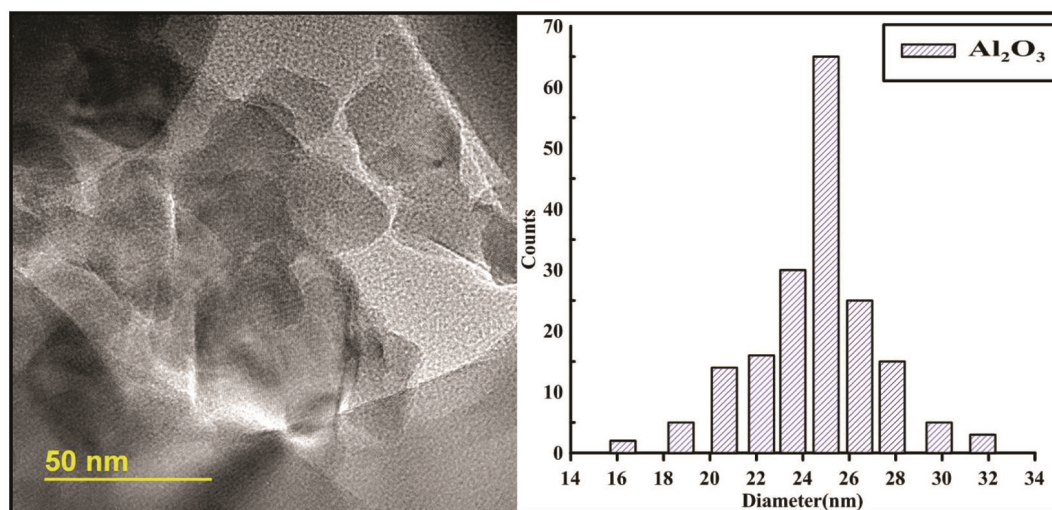
Figure 1. Transmission electron micrograph and particle distribution of Al$_2$O$_3$ nanoparticles.
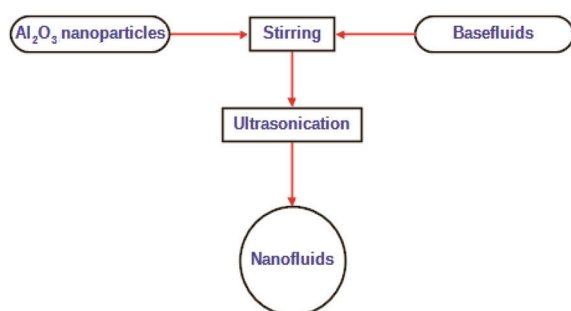
Figure 2. Schema diagram of two-step preparation process of nanofluids.

Figure 1. The nanoparticles are near spherical and heavily agglomerated. Their size varies in the range of 15–45 nm with a maximum existence at 25 nm.

Preparation and stabilization of nanofluids

Preparation is crucial for applying NFs in heat transfer augmentation. Generally, single-step or two-step process is applied to produce NFs. Two-step process is the most successful and economical method for preparing NFs containing oxide nanoparticles[11]. Hence, in this experiment, Al$_2$O$_3$ NF was prepared by two-step method. The formulation process is shown in Figure 2. NFs are prone to sedimentation. Therefore, they need special treatments to make them evenly stable and durable suspension with negligible aggregation and no chemical change. Generally, pH change, surfactant addition and ultrasonication are used to provide stability in NFs. In this experiment, surfactant was not used during preparation since the application of surfactants has some issues such as foam formation, change of purity of NFs, etc.[12]. Ultrasonication was used here to break the nanoparticle aggregates and to provide better stability. Al$_2$O$_3$ nanoparticles were directly mixed with water using a magnetic stirrer and then put into an ultrasonic cleaner (LabmanScientific Instruments, India) having 50 W capacity with an operating frequency of 40 ± 3 kHz for 3 h. The sonication energy dissipates heat energy that further elevates the temperature of the samples. The rise in temperature causes vapourization of basefluids causing change in the concentration of NF. Therefore, a water bath was employed to maintain the temperature of the test samples at room temperature (25°C). NF at different weight fractions of 0.01–1% was prepared by changing the weight of added nanoparticles in basefluid. A digital weighing scale, having an accuracy of ± 0.0001 g, was utilized to measure the weight of nanoparticles. Figure 3 displays the prepared NF samples, those showed slight sedimentation even after 7 days.

Figure 4 illustrates the particle size distributions in various concentrations of NF that were obtained by dynamic light scattering (DLS) analysis using Malvern Zetasizer (Malvern Instruments, UK) at 173°C back scattering angle. DLS estimates the hydrodynamic size or cluster
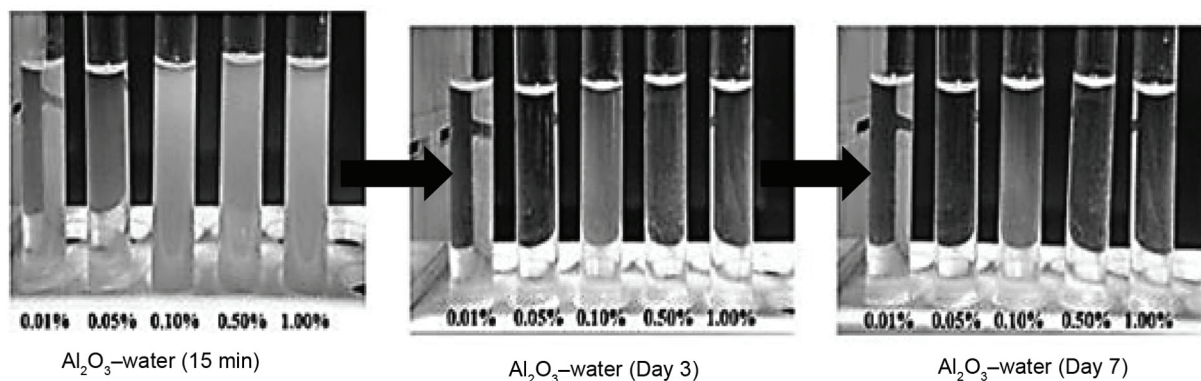
Figure 3. Sedimentation photographs of Al₂O₃–water NF.
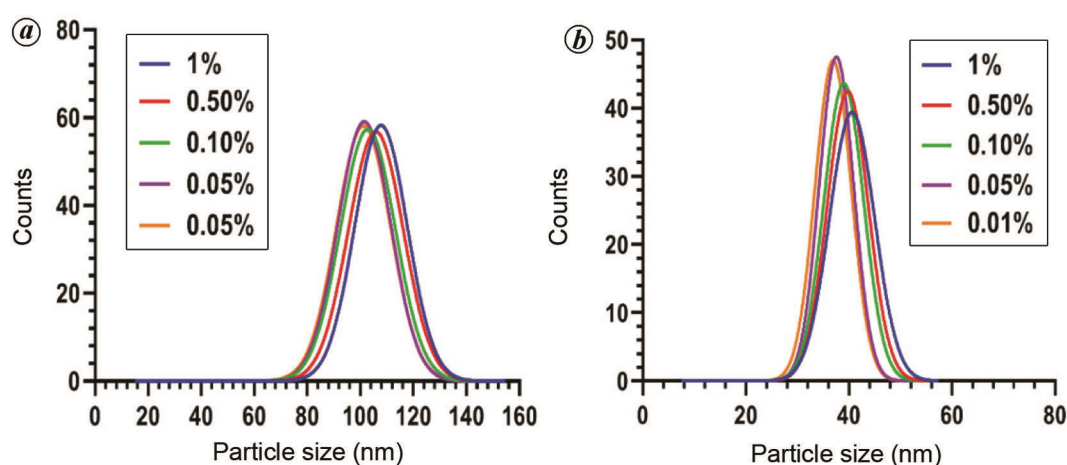
Figure 4. Particle size distribution of Al₂O₃–water NF samples by dynamic light scattering analysis.

size of nanoparticles using light scattering property of nanoparticles as a result of Brownian motion in dispersed phase[13]. This method is also suitable to detect the stability of NFs. The mean particle size in freshly prepared NF samples varied from 98.5 nm to 110.3 nm and the size range reduced to 37.12 nm to 41.28 nm after 7 days. This indicates sedimentation in NFs leaving the smaller particles easily detected by the instrument[3].

Measurement of thermal conductivity

The thermal conductivity of Al₂O₃ NF was measured using a thermal conductivity meter (Mittal Enterprises, India). A schematic view of the instrument is given in Figure 5.

The working of the apparatus is based on the heat conduction owing to the hydro-acoustic vibrations in fluids. The thermal conductivity of NF is measured from sound velocity using the modified Bridgman equation[14]. The equations involved in the thermal conductivity calculation are provided as follows

$$v = \lambda \times f. \tag{1}$$

Bridgman[14] established a mathematical formula which correlates thermal conductivity with sound velocity as mentioned in eq. (2)

$$k = 3v \left(\frac{N}{V} \right)^{2/3} K_B. \tag{2}$$

Later, Hemalatha[15] modified the Bridgman's equation as presented in eq. (3)

$$k_{nf} = 2.8v \left(\frac{N}{V_{nf}} \right)^{2/3} K_B. \tag{3}$$

where v, λ and f are ultrasonic velocity, wavelength of standing wave, frequency respectively; k the thermal conductivity; N, V and K_B stand for Avogadro number (6.023×10^{23}), molar volume and Boltzmann Constant (1.3807×10^{-23} J/K) respectively, and nf denotes nanofluid.

The thermal conductivity meter (as shown in Figure 5) is equipped with a stainless steel made cylindrical test-cell. Ultrasonic waves of known frequency, released by a piezoelectric crystal located at the base of the apparatus

passes through the test-cell. Standing waves are formed by the back and forth movement of a reflector. The movement of the reflector is controlled by the rotation of the spindle of a digital micrometer (±0.001 mm accuracy) mounted at the top of the test-cell. The wavelengths of the standing waves were recorded from micrometer reading corresponding to the highest deflections in current reading. The Al_2O_3 NFs thermal conductivity was calculated using the eqs (3) and (4). The test-cell temperature was controlled at different level by an external peripheral flow of hot water originated from isothermal laboratory bath having an accuracy of ±0.1°C. Thermal conductivity values of NF with 0.01%–1 wt% were measured over the temperature range of 25–65°C.

Experimental uncertainty

Each experimental run was carried out six times and it is presented here as mean ± standard deviation. The standard deviation in a set of measurements was estimated using eq. (4).

$$\sigma = \sqrt{\frac{\sum_i (k - \bar{k})^2}{n^2}},$$ (4)

where k is the thermal conductivity, $\bar{k}$ average of the thermal conductivity measurements and n is the number of experimental runs.

The measurement of uncertainty (U) in the thermal conductivity experiment was carried out using the following formula

$$U = \pm \sqrt{\left(\frac{\Delta k}{k}\right)^2 + \left(\frac{\Delta w}{w}\right)^2 + \left(\frac{\Delta t}{t}\right)^2}.$$ (5)
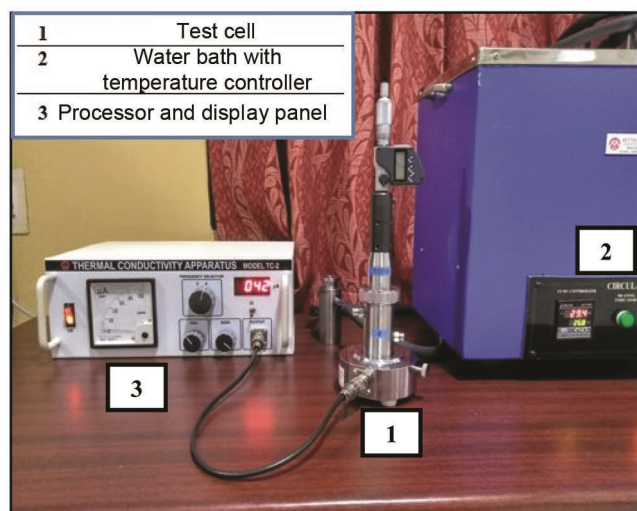
Figure 5. View of the thermal conductivity meter[27].

The highest uncertainty obtained in the thermal conductivity measurement was ±3.21%.

Results and discussion

Experimental validation

To confirm the validity of the present experiment, obtained thermal conductivity data of DI water was compared with National Institute of Standards and Technology (NIST)[16] data over 25–65°C at 10°C interval, and are presented in Table 2. As shown in Table 2, the maximum deviation between experimental and standard data is in a tolerable range of 1.10%. Hence, it proved the accuracy of the measurements.

Effects of concentration and temperature on thermal conductivity

Thermal conductivity data of Al_2O_3 NFs were calculated using the sonic velocities and they are presented in Table 3. It is clear from Table 3 that the sound velocity increases with temperature as well as concentration. As mentioned earlier, the instrument accounts hydro-acoustic vibration, which was improved by temperature rise due to heat input. Moreover, increase in particle addition also boosted the frequency of nanoparticle collision, which further enhanced Phonon vibration in supernatant particles. As a result, the velocity of sound increased.

The impacts of weight fraction and temperature on the thermal conductivity of NFs are presented in Figure 6. As shown in Figure 6, the thermal conductivity of Al_2O_3 NF improves almost linearly with the rise in weight fraction at various temperatures. Paul *et al.*[17] also discovered a similar tendency in the TCE of ethylene glycol using $Al_{95}Zn_{05}$ nanoparticles.

Table 2. Validation data for present experiment

Temperature (°C)	Thermal conductivity ($Wm^{-1} K^{-1}$)		
	NIST data	Experimental data	Deviation (%)
25	0.607	0.605	0.33
35	0.623	0.619	0.64
45	0.637	0.644	−1.10
55	0.649	0.655	−0.92
65	0.655	0.659	0.61

Table 3. Sound velocity in Al_2O_3–water NFs at studied weight fraction and temperatures

Temperature (°C)	Sound velocity (m/s)				
	1%	0.50%	0.10%	0.05%	0.01%
25	1535	1530	1525	1520	1515
35	1584	1579	1574	1569	1564
45	1631	1624	1619	1614	1609
55	1675	1670	1665	1660	1655
65	1714	1709	1705	1701	1697

The mixing of nanoparticles of very high thermal conductivity caused an extensive increase in the thermal conductivity of basefluid. In addition, particle interactions became more frequent with a rise in concentration that further influenced the thermal conductivity increment.

The effect of temperature also influenced the thermal conductivity as shown in Figure 6. The temperature elevation caused thermal conductivity increments in NF samples of various concentrations. The increase in Brownian motion due to a rise in temperature causes better heat diffusion. Consequently, the test samples showed a TCE with temperature rise. The present results are similar to the published reports[18–21]. Therefore, concentrated NFs at elevated temperatures are potent for various heat transfer applications.

The amount of enhancement in thermal conductivity of basefluid (k_{bf}) by dispersion of nanoparticles can be estimated as thermal conductivity ratio (k_r) expressed as below

$$k_r = \frac{k_{nf}}{k_{bf}}. \tag{6}$$

Figure 7 depicts the k_r values plotted as a function of concentration and temperature. It is clear from this figure that the k_r values of Al_2O_3 NF increase nonlinearly by increasing weight fraction as well as temperature. The nonlinear enhancement points towards several nanoscale phenomena such as Brownian motion, micro-convection, particle interactions that are the sole mechanisms behind TCE in NFs. It was also clear that an attractive rise in k_r was not observed at low temperature and low concentration due to a lower number of particle contacts and a lack of mobility[22]. The experimental results of $k_r > 1$ suggested that NF had higher heat transfer capability than their basefluid.

Comparison with classical models

The experimental outcome of the thermal conductivity were compared with the predicted data by Maxwell's model[23] and Hamilton–Crosser model (H–C model)[24] at 25°C. The comparison is presented in Figure 8. The comparison demonstrates that the classical models are unable to predict the current experimental findings. Such an augmentation is prevalent in the data because conventional models do not take into account the micro-scale processes that drive the thermal conductivity improvement in NF[25].
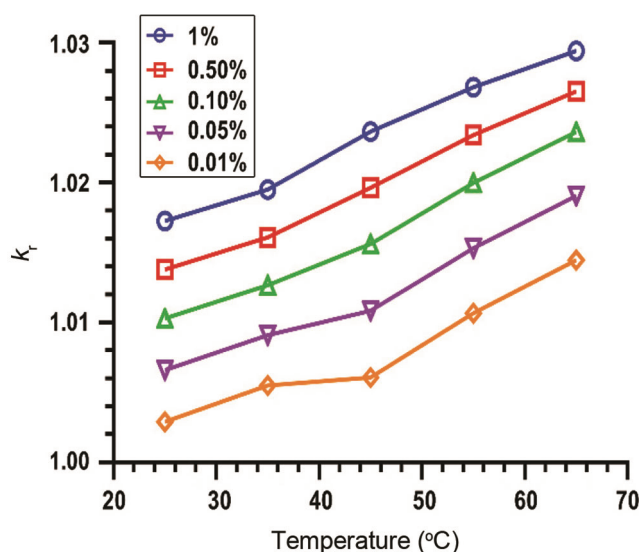
Figure 7. k_r values of Al_2O_3–water NF at different weight fractions and temperatures.

Figure 6. Thermal conductivity of Al_2O_3 NFs at different weight fractions and temperatures.
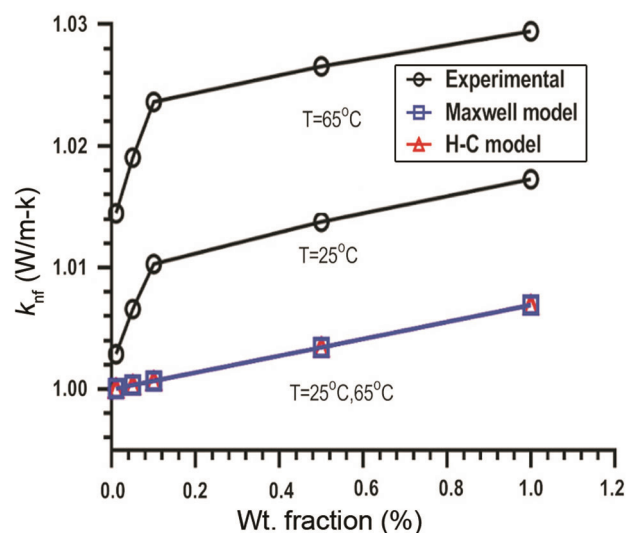
Figure 8. Comparison of experimental thermal conductivity data with theoretical predictions.
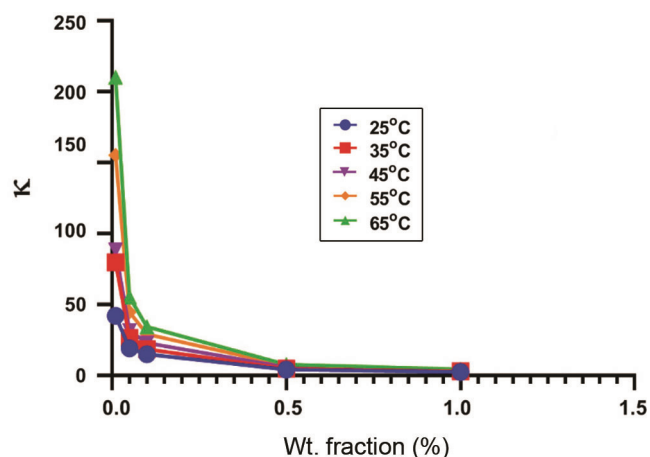
Figure 9. Excess thermal conductivity coefficient (κ) values at different concentrations and temperatures.

Excess thermal conductivity coefficient

For additional investigation of TCE in NF, Keblinski et al.[26] proposed an idea of excess TCE coefficient (κ), defined as

$$\kappa = \frac{k_r - 1}{k_{r,HC} - 1}. \tag{7}$$

From the above definition of κ, it is the ratio of experimental measurement of TCE to the TCE measured by H–C model. If $\kappa = 1$, then the measurement agrees with classical macroscopic theories, and if $\kappa > 1$ then TCE is according to the micro- or nanoscale theories such as Brownian movement, micro-convection, thermophoresis, etc. The κ values measured using experimental data and with the H–C model are presented in Figure 9. The κ values are all >1 which indicates the enhancement in thermal conductivity follows nano- or microscale theories. Therefore, it is again proved that classical theories are incapable of describing TCE in NFs. Moreover, from Figure 9, it can be seen that κ decreases with concentration rise, whereas, it increases with temperature elevation. Therefore, it appears that the influence of temperature dominates the effect of particle inclusion in NFs. This finding is quiet interesting because, the value is expected to grow with concentration as well as temperature increase. One probable explanation for this phenomenon is that particle inclusion produces greater sedimentation in NFs, resulting in a decrease in TCE.

Conclusion

(a) Two-step process was applied to formulate Al_2O_3–water NF. The sedimentation photographs of NF and DLS analysis show good dispersion behaviour and decent stability of NFs.

(b) The thermal conductivity of NF is strongly impacted by the changes in weight fraction and temperature. The increase in thermal conductivity in NF maintains a linear connection between concentration and temperature.

(c) Augmentation in the thermal conductivity of NF compared to its basefluid (k_r) follows a nonlinear pattern as concentration and temperature rise. This hints at the nano- or microscale processes, which cause thermal conductivity augmentation in such fluids.

(d) The experimental thermal conductivity data are not in agreement with well-established classical models.

(e) The excess thermal conductivity coefficient shows discrepancies between experimental thermal conductivity data and theoretical models. The TCE in NF is controlled by the micro-nanoscale phenomena, which are indescribable by general micro-scale theories.

(f) Particle inclusion brings about TCE in NFs and at the same time sedimentian enhancement in NFs. Therefore, NFs of too low or too high concentration should be avoided. Thus, an optimization study in this regard is recommended as the outlook of this study.

Conflict of interests: The authors declare that there is no conflict of interest.

1. Paul, G., Das, P. K. and Manna, I., Assessment of the process of boiling heat transfer during rewetting of a vertical tube bottom flooded by alumina nanofluid. *Int. J. Heat Mass Transf.*, 2016, **94**, 390–402.
2. Choi, S. U. S. and Eastman, J. A., *Enhancing Thermal Conductivity of Fluids with Nanoparticles* (No. ANL/MSD/CP-84938; CONF-951135-29), Argonne National Lab., IL United States, 1995.
3. Ali, N., Teixeira, J. A. and Addali, A., A review on nanofluids: fabrication, stability and thermophysical properties. *J. Nanomater.*, 2018, **2018**, 6978130.
4. Eastman, J. A., Choi, S. U. S., Li, S., Yu, W. and Thompson, L. J., Anomalously increased effective thermal conductivities of ethylene glycol-based nanofluids containing copper nanoparticles. *Appl. Phys. Lett.*, 2001, **78**, 718–720.
5. Choi, S. U. S., Zhang, Z. G., Yu, W., Lockwood, F. E. and Grulke, E. A., Anomalous thermal conductivity enhancement in nanotube suspensions. *Appl. Phys. Lett.*, 2001, **79**, 2252–2254.
6. Tawfik, M. M. *et al.*, Experimental studies of nanofluid thermal conductivity enhancement and applications: a review. *Renew. Sustain. Energy Rev.*, 2017, **75**, 1239–1253.
7. Paul, G., Chopkar, M., Manna, I. and Das, P. K., Techniques for measuring the thermal conductivity of nanofluids: a review. *Renew. Sustain. Energ. Rev.*, 2010, **14**, 1913–1924.
8. Haghighi, E. B. *et al.*, Shelf stability of nanofluids and its effect on thermal conductivity and viscosity. *Measur. Sci. Technol.*, 2013, **24**, 105301.
9. Shahsavar, A., Saghafian, M., Salimpour, M. R. and Shafii, M. B., Effect of temperature and concentration on thermal conductivity and viscosity of ferrofluid loaded with carbon nanotubes. *Heat Mass Transf.*, 2016, **52**, 2293–2301.
10. Sridhara, V. and Satapathy, L. N., Al_2O_3-based nanofluids: a review. *Nanoscale Res. Lett.*, 2011, **6**, 456.
11. Manna, I., Synthesis, characterization and application of nanofluid – an overview. *J. Indian Inst. Sci.*, 2012, **89**, 21–33.
12. Mukherjee, S., Mishra, P. C. and Chaudhuri, P., Stability of heat transfer nanofluids – a review. *ChemBioEng Rev.*, 2018, **5**, 312–333.

13. Berne, B. J. and Pecora, R., *Dynamic Light Scattering: with Applications to Chemistry, Biology and Physics*, Dover Publication, Inc., New York, 2000.

14. Bird, R. B., Transport phenomena. *Appl. Mech. Rev.*, 2002, **55**, R1–R4.

15. Rashin, M. N. and Hemalatha, J., A novel ultrasonic approach to determine thermal conductivity in cuo–ethylene glycol nanofluids. *J. Mol. Liq.*, 2014, **197**, 257–262.

16. Lemmon, E. W., Huber, M. L. and McLinden, M. O., Nist standard reference database 23, reference fluid thermodynamic and transport properties (refprop), version 9.0, National Institute of Standards and Technology. R1234yf fld file dated December 2010, **22**.

17. Paul, G., Philip, J., Raj, B., Das, P. K. and Manna, I., Synthesis, characterization, and thermal property measurement of nano-al95zn05 dispersed nanofluid prepared by a two-step process. *Int. J. Heat Mass Trans.*, 2011, **54**, 3783–3788.

18. Issa, R. J., Effect of nanoparticles size and concentration on thermal and rheological properties of Al_2O_3–water nanofluids. In Proceedings of the World Congress on Momentum, Heat and Mass Transfer (MHMT'16), 2016, pp. 4–5.

19. Buonomo, B., Manca, O., Marinelli, L. and Nardini, S., Effect of temperature and sonication time on nanofluid thermal conductivity measurements by nano-flash method. *Appl. Therm. Eng.*, 2015, **91**, 181–190.

20. Patel, H. E., Das, S. K., Sundararajan, T., Nair, A. S., George, B. and Pradeep, T., Thermal conductivities of naked and monolayer protected metal nanoparticle based nanofluids: manifestation of anomalous enhancement and chemical effects. *Appl. Phys. Lett.*, 2003, **83**, 2931–2933.

21. Shukla, R. K. and Dhir, V. K., Effect of Brownian motion on thermal conductivity of nanofluids. *J. Heat Transf.*, 2008, **130**(4), 042406.

22. Esfe, M. H., Arani, A. A. A., Badi, R. S. and Rejvani, M., Ann modeling, cost performance and sensitivity analysing of thermal conductivity of DWCNT–SiO_2/EG hybrid nanofluid for higher heat transfer. *J. Therm. Anal. Calorim.*, 2018, **131**, 2381–2393.

23. Mehta, S., Chauhan, K. P. and Kanagaraj, S., Modeling of thermal conductivity of nanofluids by modifying Maxwell's equation using cell model approach. *J. Nanopart. Res.*, 2011, **13**, 2791–2798.

24. Hamilton, R. L. and Crosser, O. K., Thermal conductivity of heterogeneous two-component systems. *Ind. Eng. Chem. Fund.*, 1962, **1**, 187–191.

25. Gandhi, K. S., Thermal properties of nanofluids: controversy in the making? *Curr. Sci.*, 2007, **92**, 717–718.

26. Keblinski, P., Phillpot, S. R., Choi, S. U. S. and Eastman, J. A., Mechanisms of heat flow in suspensions of nano-sized particles (nanofluids). *Int. J. Heat Mass Transf.*, 2002, **45**, 855–863.

27. Mukherjee, S., Panda, S. R., Mishra, P. C. and Chaudhuri, P., Enhancing thermophysical characteristics and heat transfer potential of TiO_2/water nanofluid. *Int. J. Thermophys.*, 2021, **41**, 1–33.